FEM modelling and simulation of thixo-viscoplastic flow problems

Naheed Begum, Abderrahim Ouazzi, Stefan Turek
Institute for Applied Mathematics, LS III, TU Dortmund University, D-44227 Dortmund, Germany
Naheed.Begum@math.tu-dortmund.de,
Abderrahim.Ouazzi@math.tu-dortmund.de
Stefan.Turek@math.tu-dortmund.de

Keywords: Thixo-viscoplastic, Rejuvenation, Aging, FEM, Newton-multigrid, LPSC

ABSTRACT

Oberseminar, a platform for brain-sharing through a true discussion with colleagues, we base today conversation on talk concerning our recent research about thixotropy in flow problems.

We will present FEM quasi-Newtonian modelling and simulation for thixo-viscoplastic flows, as straightforward way to generalize the standard FEM settings of Navier-Stokes equations. The structure parameter is integrated within the nonlinear viscosity as a feedback response for the evolution process of competition between breakdown and buildup inhabited in thixotropic material.

Firstly, we provide wellposedness results for TVP problem, followed by establishing the best approximation, then introducing higher order stabilized FEM approximations to enhance the discrete weak energy norm to an equivalent one-norm. In fact, the energy inequality presents some coarseness in terms of proportional dependency of its constants on regularization parameter, nonoptimality estimate for microstructure, and extra regularity requirement for velocity.

Secondly, we solve the discrete nonlinear system using new TVP Newton's monolithic geometric multigrid solver. The solver is robust w.r.t. regularization, as a must for obtaining accurate solutions for quasi-Newtonian modelling of TVP problem.

Lastly, we revisit Couette flow and 4:1 contraction flow by activating thixotropy. For the former, we correlate the constitutive models of shear rate independent and shear rate dependent stress via material microstructure, to enable analysis of type of transitions between solid-like and fluid-like regimes. For 4:1 contraction flow, we show that thixotropy induces extra breakdown layers in the vicinity of walls, which allows optimization of restart pressure in pipelines. Consequently, we are replicating phenomenological process of competition of breakdown/rejuvenation and buildup/aging characteristics of thixotropic material in terms of localization and shear banding.

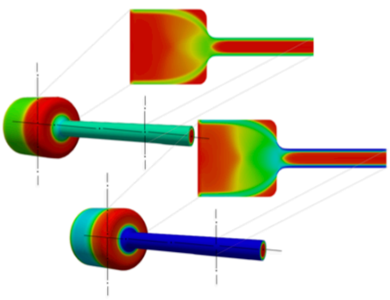

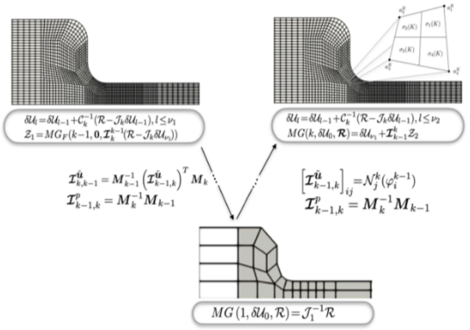

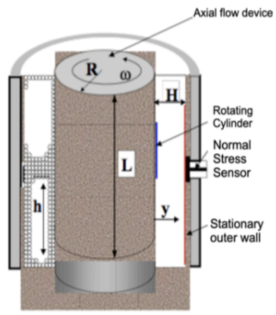

nota bene: The material of this talk is based on our below recent work;

[1] Ouazzi, A., Begum, N., Turek, S. Newton-Multigrid FEM Solver for the Simulation of Quasi-Newtonian Modeling of Thixotropic Flows, 700, *Numerical Methods and Algorithms in Science and Engineering*, 2021.

[2] Begum, N., Ouazzi, A., Turek, S. Finite Element Methods for the simulation of thixotropic flow problems.*9th edition of the ICCM for Coupled Problems in Science and Engineering*, 2021.

[3] Begum, N., Ouazzi, A., Turek, S. Monolithic Finite Element method for the simulation of thixo-viscoplastic flows. *Book of Extended Abstracts of the 6th Eccomas Young Investigators Conference*, 2021.

[4] Begum, N., Ouazzi, A.,Turek, S. Monolithic Newton-multigrid FEM for the simulation of thixotropic flow problems. *(GAMM), Wiley-Interscience*, https://doi.org/10.1002/pamm.202100019, 2021.

[5] Begum, N., Ouazzi, A.,Turek, S. FEM Simulations for Thixo-viscoplastic Flow Problems; Wellposedness Results,*Fakultät für Mathematik, TU Dortmund University, Technical report*: 653, 2022.

[6] Begum, N., Ouazzi, A.,Turek, S. FEM Simulations for Thixo-viscoplastic Flow Problems: Error Analysis, *Fakultät für Mathematik, TU Dortmund University, Technical report*: 656, 2022.

FEM modelling and simulation of thixo-viscoplastic flow problems

Naheed Begum, Abderrahim Ouazzi, Stefan Turek
Institute of Applied Mathematics, LS III,
TU Dortmund University, Dortmund, Germany

Oberseminar 2022,
5th December 2022, Dortmund, Germany

fakultät für mathematik

lehrstuhl für angewandte mathematik und numerik

Motivation

Why "Thixotropy"?

- **Processing of thixotropic materials relevant for industrial applications**

➡ **Lubrication, asphalt, self-compacting concrete…**

- **Physically fascinating due to improved mechanical properties**

Goal:

- **Modern CFD methods with high accuracy, robustness and efficiency for thixotropic materials**

➡ **Saving time, money and resources**

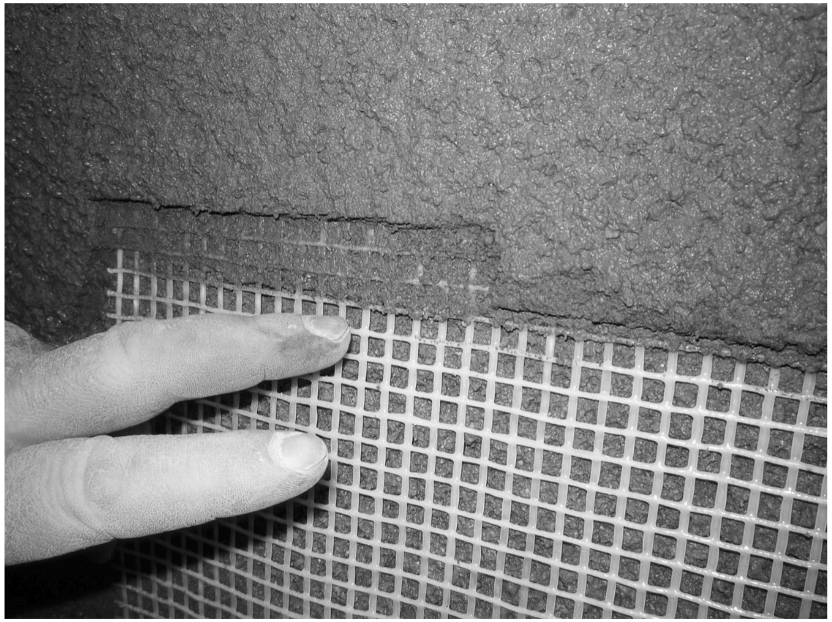

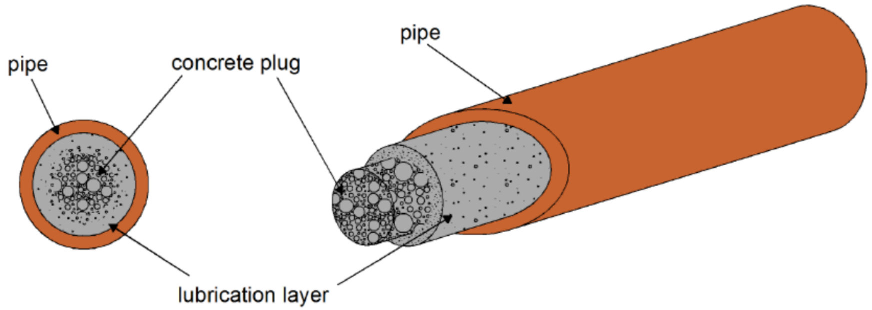

Investigation of buildup and breakdown competitive process in thixoviscoplastic materials

Thixotropy in flow problems

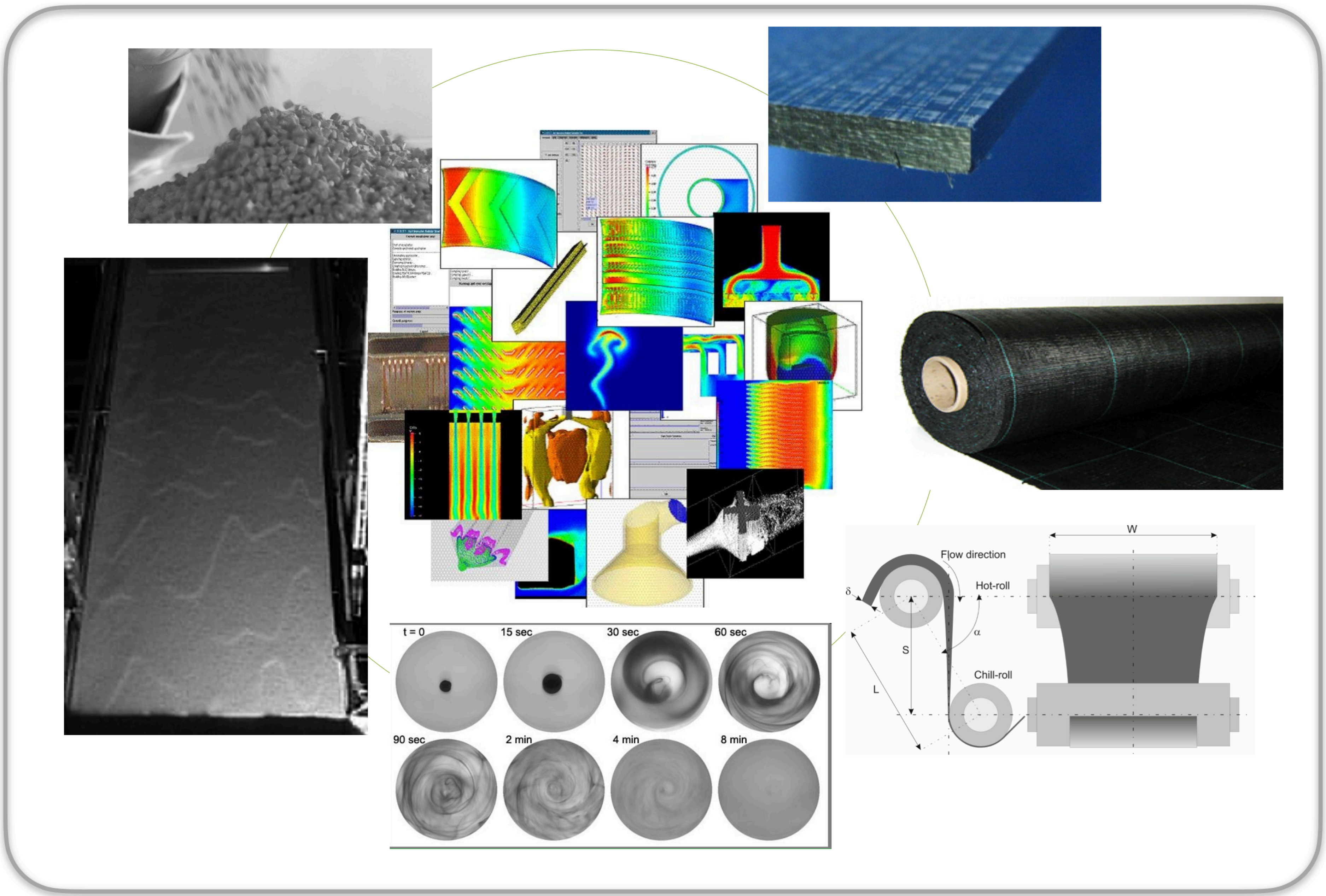

Thixoviscoplastic stress

$$\begin{cases} \boldsymbol{\sigma} = 2\,\eta(D_{\mathrm{II}},\lambda)\boldsymbol{D}(\boldsymbol{u}) + \sqrt{2}\,\tau(\lambda)\dfrac{\boldsymbol{D}(\boldsymbol{u})}{\sqrt{D_{\mathrm{II}}}} & \text{if } D_{\mathrm{II}} \neq 0 \\ \sigma_{\mathrm{II}} \leq \tau(\lambda) & \text{if } D_{\mathrm{II}} = 0 \end{cases}$$

Microstructure evolution equation

$$\left(\frac{\partial}{\partial t} + \boldsymbol{u}\cdot\nabla\right)\lambda + \mathcal{M}(D_{\mathrm{II}},\lambda) = f_\lambda$$

Thixotropic models

$$\mathcal{M} = \mathcal{G} - \mathcal{F}$$

	η	τ	$\mathcal{F}$	$\mathcal{G}$
Worrall et al.	$\lambda\,\eta_0$	τ_0	$\mathcal{M}_a(1-\lambda)\,\lVert\mathbf{D}\rVert$	$\mathcal{M}_b\lambda\,\lVert\mathbf{D}\rVert$
Coussot et al.	$\lambda^g\,\eta_0$		$\mathcal{M}_a$	$\mathcal{M}_b\lambda\,\lVert\mathbf{D}\rVert$
Houška	$(\eta_0+\eta_\infty\lambda)\,\lVert\mathbf{D}\rVert^{n-1}$	$(\tau_0+\tau_\infty\lambda)$	$\mathcal{M}_a(1-\lambda)$	$\mathcal{M}_b\lambda^m\,\lVert\mathbf{D}\rVert$
Mujumbar et al.	$(\eta_0+\eta_\infty\lambda)\,\lVert\mathbf{D}\rVert^{n-1}$	$\lambda^{g+1}G_0\Lambda_c$	$\mathcal{M}_a(1-\lambda)$	$\mathcal{M}_b\lambda\,\lVert\mathbf{D}\rVert$
Dullaert et al.	$\lambda\eta_0$	$\lambda G_0(\lambda\,\lVert\mathbf{D}\rVert)\Lambda_c$	$(\mathcal{M}_{a_1}+\mathcal{M}_{a_2}\,\lVert\mathbf{D}\rVert)(1-\lambda)t^p$	$\mathcal{M}_b\lambda\,\lVert\mathbf{D}\rVert\,t^{-p}$

Quasi-Newtonian TVP modelling

➢ Viscosity model for TVP flow

- **Classical approximations**

$$\begin{cases} I. & \dfrac{1}{\sqrt{D_{\mathrm{II},r}}} := \dfrac{1}{\sqrt{(D_{\mathrm{II}} + (k^{-1})^2)}} \\ II. & \dfrac{1}{\sqrt{D_{\mathrm{II},r}}} := \dfrac{1}{\sqrt{D_{\mathrm{II}}}} \left(1 - e^{-k\sqrt{D_{\mathrm{II}}}}\right) \end{cases}$$

- **Extended viscosity defined on all domain**

$$\mu(D_{\mathrm{II},r}, \lambda) = \eta(D_{\mathrm{II}}, \lambda) + \tau(D_{\mathrm{II}}, \lambda) \frac{\sqrt{2}}{2} \frac{1}{\sqrt{D_{\mathrm{II},r}}}$$

➢ Full set of equations

$$\begin{cases} \left(\dfrac{\partial}{\partial t} + \boldsymbol{u} \cdot \nabla\right) \boldsymbol{u} - \nabla \cdot \left(2\mu(\boldsymbol{D}_{\mathrm{II},r}, \lambda)\boldsymbol{D}(\boldsymbol{u})\right) + \nabla p = \boldsymbol{f_u} & \text{in } \Omega \\ \nabla \cdot \boldsymbol{u} = 0 & \text{in } \Omega \\ \left(\dfrac{\partial}{\partial t} + \boldsymbol{u} \cdot \nabla\right) \lambda + \mathcal{M}(D_{\mathrm{II}}, \lambda) = f_\lambda & \text{in } \Omega \end{cases}$$

- **Flow variables** $(\lambda, \boldsymbol{u}, p)$
  - **Set** $\mathbb{T} := H^1_{\Gamma^-}(\Omega), \mathbb{V} := \left[H^1_0(\Omega)\right]^2, \mathbb{Q} := L^2(\Omega), \mathbb{W} := \mathbb{T} \times \mathbb{V}$
  - **Set** $\tilde{\boldsymbol{u}} := (\lambda, \boldsymbol{u})$
  - **Find** $(\lambda, \boldsymbol{u}, p) \in \mathbb{T} \times \mathbb{V} \times \mathbb{Q}$ **s.t.**

$$\left\langle \mathcal{K}(\lambda, \boldsymbol{u}, p), (\xi, \boldsymbol{v}, q) \right\rangle = \left\langle \mathcal{L}, (\xi, \boldsymbol{v}, q) \right\rangle, \quad \forall (\xi, \boldsymbol{v}, q) \in \mathbb{T} \times \mathbb{V} \times \mathbb{Q}$$

Theorem [Begum et al. 2022a]

Let $\boldsymbol{f_u} \in (L^2(\Omega))^2$ and $f_\lambda \in L^2(\Omega)$, the thixo-viscoplastic problem has a unique solution $(\tilde{\boldsymbol{u}}, p) = (\lambda, \boldsymbol{u}, p) \in \mathbb{W} \times \mathbb{Q}$ with the following bound on data

$$\|\boldsymbol{u}\|_1 \leq \frac{1}{\eta_0 \mathcal{C}_K} \|\boldsymbol{f_u}\|_0$$

$$\mathcal{M}_a \|\lambda\|_0^2 + \frac{1}{2} \langle \lambda \rangle^2 \leq \frac{1}{\mathcal{M}_a} \|f_\lambda\|_0^2$$

$$\|p\|_0 \leq \frac{1}{\beta} \left(1 + \frac{2\,(\eta_\infty + k\tau_\infty) + |\boldsymbol{u}|_1}{\eta_0 \mathcal{C}_K}\right) \|\boldsymbol{f_u}\|_0$$

with $\mathcal{C}_K$ denotes Korn's inequality constant.

Coercivity in weaker norm for the microstructure !
Pressure is underdertmined in rigid zone !

Approximated TVP problem

technische universität dortmund

- **Conforming approximations**

$$\mathbb{T}_h \subset \mathbb{T},\ \mathbb{V}_h \subset \mathbb{V},\ \mathbb{Q}_h \subset \mathbb{Q},\ \mathbb{W}_h := \mathbb{T}_h \times \mathbb{V}_h \text{ , and } \mathcal{A}_{\tilde{\mathbf{u}}h} = \mathcal{A}_{\tilde{\mathbf{u}}},\ \mathcal{B}_h = \mathcal{B}$$

➢ **Find** $(\lambda_h, \boldsymbol{u}_h, p_h) \in \mathbb{T}_h \times \mathbb{V}_h \times \mathbb{Q}_h$ **s.t**

$$\Big\langle \mathcal{K}(\lambda_h, \boldsymbol{u}_h, p_h), (\xi_h, \boldsymbol{v}_h, q_h) \Big\rangle = \Big\langle \mathcal{L}, (\xi_h, \boldsymbol{v}_h, q_h) \Big\rangle,\ \ \forall (\xi_h, \boldsymbol{v}_h, q_h) \in \mathbb{T}_h \times \mathbb{V}_h \times \mathbb{Q}_h$$

Theorem [Begum et al. 2022b]

Let $\boldsymbol{f_u} \in (L^2(\Omega))^2$ *and* $f_\lambda \in L^2(\Omega)$*, the approximate thixo-viscoplastic problem has a unique solution* $(\tilde{\mathbf{u}}_h, p_h) = (\lambda_h, \boldsymbol{u}_h, p_h) \in \mathbb{W}_h \times \mathbb{Q}_h$ *with the following a priori best approximation*

$$\|\lambda - \lambda_h\|_0^2 \ \le\ (2 + 2\tilde{\mathcal{C}}_{\lambda,\lambda}) \inf_{\xi_h \in \mathbb{T}_h} \|\lambda - \xi_h\|_1^2 + \tilde{\mathcal{C}}_{\lambda,\boldsymbol{u}} \inf_{\boldsymbol{v}_h \in \mathbb{V}_h} |\boldsymbol{u} - \boldsymbol{v}_h|_{1,\infty}^2$$

$$|\boldsymbol{u} - \boldsymbol{u}_h|_{1,\infty}^2 \le \tilde{\mathcal{C}}_{\boldsymbol{u},\lambda} \inf_{\xi_h \in \mathbb{T}_h} \|\lambda - \xi_h\|_1^2 + (2 + 2\tilde{\mathcal{C}}_{\boldsymbol{u},\boldsymbol{u}}) \inf_{\boldsymbol{v}_h \in \mathbb{V}_h} |\boldsymbol{u} - \boldsymbol{v}_h|_{1,\infty}^2 + \mathcal{C}_{\boldsymbol{u},p} \inf_{q_h \in \mathbb{Q}_h} \|p - q_h\|_0^2$$

Remark (Finite element approximation)

- **Regularization**

$$|\boldsymbol{u} - \boldsymbol{u}_h|_1^2 \equiv \tilde{\mathcal{C}}_{\boldsymbol{u},\lambda} h^{2r} |\lambda|_{r+1} + (2 + 2\tilde{\mathcal{C}}_{\boldsymbol{u},\boldsymbol{u}}) h^{2r} |\boldsymbol{u}|_{r+1}^2 + \mathcal{C}_{\boldsymbol{u},p} h^{2r} \|p\|_r^2 \equiv \mathcal{O}(k^2 h^{2r})$$

- **Coercivity in a weaker norm**

$$\|\lambda - \lambda_h\|_0 \equiv \mathcal{O}(h^r)$$

Higher order conforming FEM

✓ **The family of conforming FEM $Q_r/Q_r/P_{r-1}^{\text{disc}}$, $r \geq 2$ for $(\lambda, \boldsymbol{u}, p)$ with stabilization**

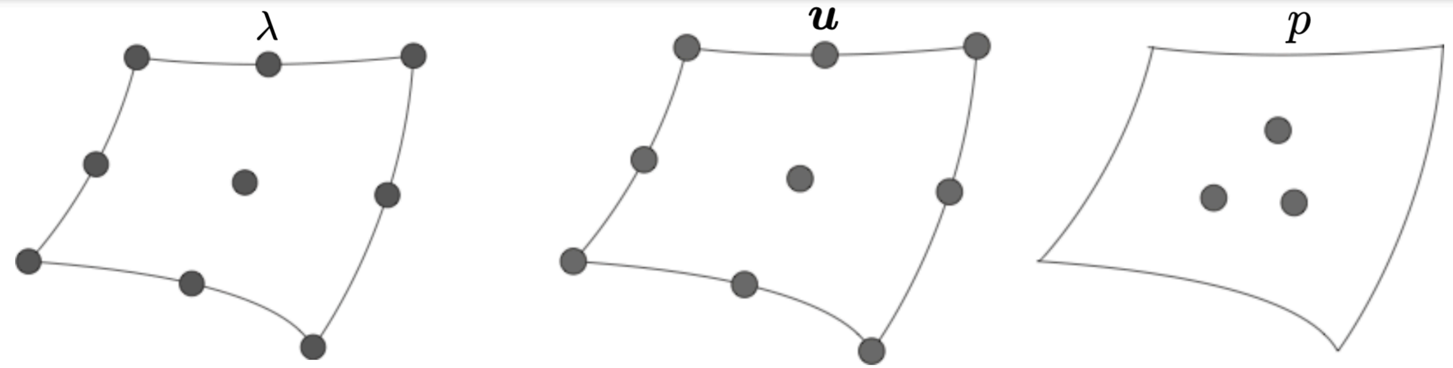

- ➢ **Inf-sup conditions is satisfied**
- ➢ **Discontinuous pressure**
  - ➢ **Practical w.r.t. monolithic approach**
  - ➢ **Element-wise mass conservation**

✓ **Highly consistent and symmetric stabilization**

$$j_\lambda(\lambda_h, \xi_h) = \sum_{e \in \mathcal{E}_h} h^2 \gamma_\lambda \int_e [\nabla \lambda_h] : [\nabla \xi_h] \, d\Omega, \quad j_{\lambda,l} := j_\lambda \text{ for } \gamma_\lambda = \text{cst.}$$

- ➢ **Coercivity in a strong norm for the microstructure eq.**
- ➢ **Reduces the regularity requirement for velocity**
- ➢ **Efficient and robust w.r.t. multigrid solver**

Coercivity in a stronger norm

$$\|\lambda\| = \left(\mathcal{M}_a \|\lambda\|_0 + \frac{1}{2} \langle \lambda \rangle^2 + j_\lambda(\lambda, \lambda) \right)^{\frac{1}{2}}$$

Theorem:

Let $\boldsymbol{f_u} \in (L^2(\Omega))^2$ *and* $f_\lambda \in L^2(\Omega)$, *the approximate thixo-viscoplastic problem has a unique solution* $(\tilde{\boldsymbol{u}}_h, p_h) = (\lambda_h, \boldsymbol{u}_h, p_h) \in \mathbb{W}_h \times \mathbb{Q}_h$ *with the following a priori best approximation*

$$\|\lambda - \lambda_h\|^2 \leq (2 + 2\tilde{\mathcal{C}}_{\lambda,\lambda}) \inf_{\xi_h \in \mathbb{T}_h} \|\lambda - \xi_h\|_1^2 + \tilde{\mathcal{C}}_{\lambda,\boldsymbol{u}} \inf_{\boldsymbol{v}_h \in \mathbb{V}_h} |\boldsymbol{u} - \boldsymbol{v}_h|_1^2 + \inf_{\xi_h \in \mathbb{T}_h} \frac{1}{2} j_{\lambda,l}(\lambda - \xi_h, \lambda - \xi_h)$$

$$|\boldsymbol{u} - \boldsymbol{u}_h|_1^2 \leq \tilde{\mathcal{C}}_{\boldsymbol{u},\lambda} \inf_{\xi_h \in \mathbb{T}_h} \|\lambda - \xi_h\|_1^2 + (2 + 2\tilde{\mathcal{C}}_{\boldsymbol{u},\boldsymbol{u}}) \inf_{\boldsymbol{v}_h \in \mathbb{V}_h} |\boldsymbol{u} - \boldsymbol{v}_h|_1^2 + \mathcal{C}_{\boldsymbol{u},p} \inf_{q_h \in \mathbb{Q}_h} \|p - q_h\|_0^2$$

Remark:

- **Regularization:** ***Higher order FEM counterbalance the regularization coarseness***

$$|\boldsymbol{u} - \boldsymbol{u}_h|_1 \equiv \mathcal{O}(k^{-1}) \implies h \leq \mathcal{O}(k^{-\frac{2}{r}})$$

- **Coercivity in a stronger norm:** ***The optimal order and regularity is recovered***

$$\|\lambda - \lambda_h\|_0 \equiv \mathcal{O}(h^{r+\frac{1}{2}})$$

Accuracy of TVP solutions

✓ **Dependency of discretization error on regularization**

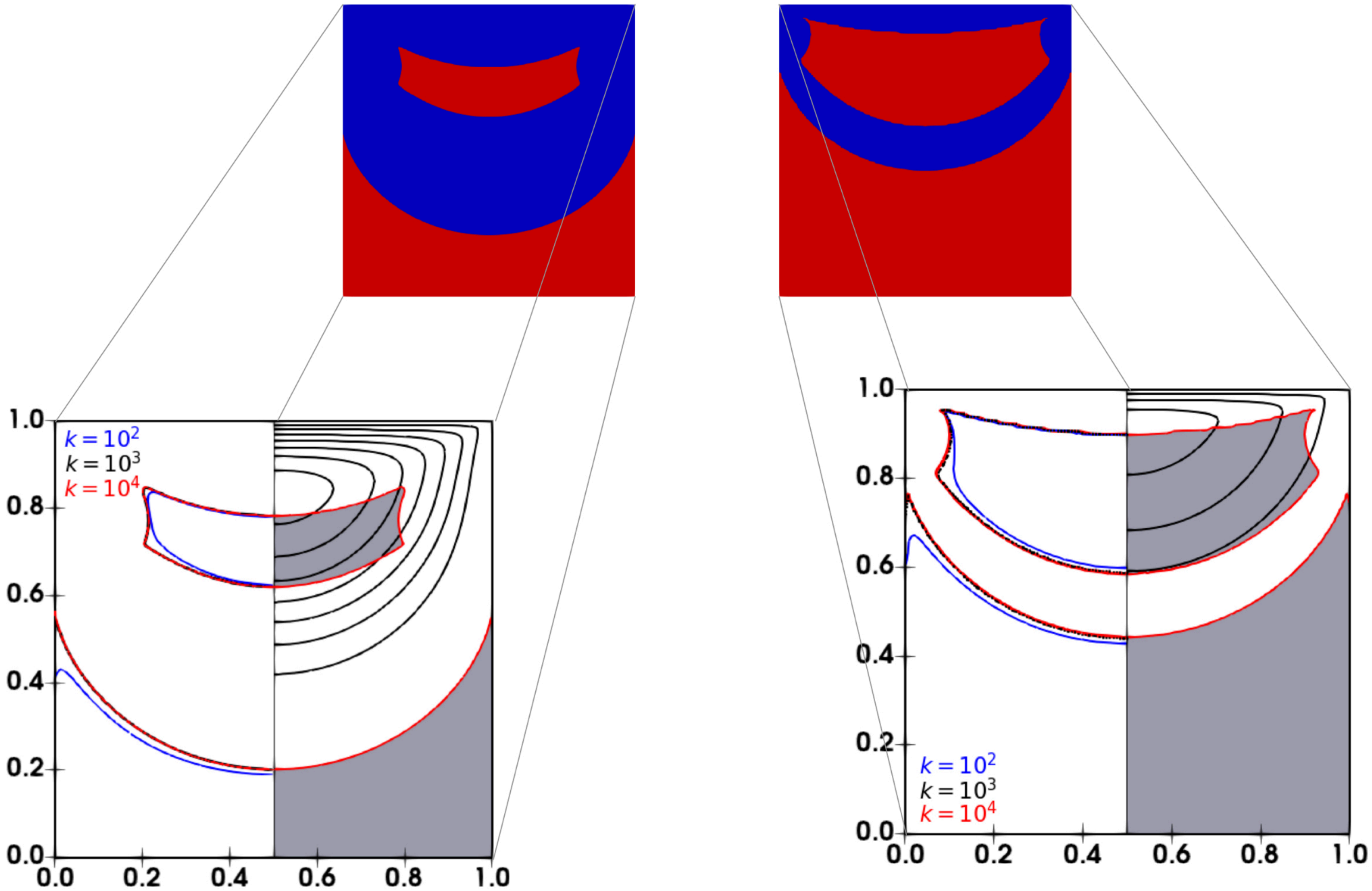

Robust solver with respect to regularization !

Global discrete Newton's method

Let $\{\varphi_i, i=1,2,\ldots,\mathtt{dim}\mathbb{W}_h\}$ and $\{\psi_i,\ i=1,\ldots,\mathtt{dim}\mathbb{Q}_h\}$ denote the basis of spaces $\mathbb{W}_h$ and $\mathbb{Q}_h$, respectively. The solution $\mathcal{U}=(\lambda,\boldsymbol{u},p)=(\tilde{\boldsymbol{u}},p)\in\mathbb{W}_h\times\mathbb{Q}_h$

$$\mathcal{U}=\sum_{i=1}^{\mathtt{dim}\mathbb{W}_h}\tilde{\boldsymbol{u}}_i\varphi_i+\sum_{i=1}^{\mathtt{dim}\mathbb{Q}_h}p_i\psi_i$$

The residuals of discrete TVP problem $\mathcal{R}(\mathcal{U})\in\mathbb{R}^{\mathtt{dim}\mathbb{W}_h+\mathtt{dim}\mathbb{Q}_h}$

$$\mathcal{R}(\mathcal{U})=(\mathcal{R}_\lambda(\lambda,\boldsymbol{u}),\mathcal{R}_{\boldsymbol{u}}(\lambda,\boldsymbol{u},p),\mathcal{R}_p(\boldsymbol{u}))=(\mathcal{R}_{\tilde{\boldsymbol{u}}}(\tilde{\boldsymbol{u}},p),\mathcal{R}_p(\boldsymbol{u}))$$

Algorithm 1: Adaptive discrete Newton

Result: $\mathcal{U}^{l+1}=\mathcal{U}^l-\omega_l\delta\mathcal{U}^l,\ \omega_l\in(0,1]$
$r_0=\|\mathcal{R}(\mathcal{U}^0)\|,\ \varepsilon_0^{\pm}$;
while $r_l\geq r_c$;
do
- (i) **Calculate convergence rate** $r_l=\frac{\|\mathcal{R}(\mathcal{U}^l)\|}{\|\mathcal{R}(\mathcal{U}^{l-1})\|}$;
- (ii) **Step-length size update** $\varepsilon_{l+1}^{\pm}=g(r_l)\varepsilon_l^{\pm}$;
- (iii) **Calculate FD Jacobian** $\left[\mathcal{J}(\mathcal{U}^l)\right]_{ij}\approx\frac{\left(\mathcal{R}_i(\mathcal{U}^l+\varepsilon_l^+\boldsymbol{e}_j)-\mathcal{R}_i(\mathcal{U}^l-\varepsilon_l^-\boldsymbol{e}_j)\right)}{\varepsilon_l^++\varepsilon_l^-}$;
- (iv) **Solve via MG** $\mathcal{J}(\mathcal{U}^l)\delta\mathcal{U}^l=\mathcal{R}(\mathcal{U}^l)$;

end

Global and blackbox !
Robustness and efficiency: Monolithic Geometric MG

Monolithic Geometric MG solver

- **Multi-level algorithm**

$$\mathcal{J}_k \delta\mathcal{U} = \mathcal{R}$$

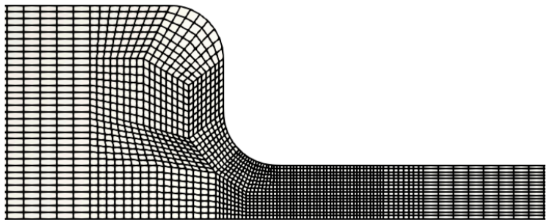

$$\delta\mathcal{U}_l = \delta\mathcal{U}_{l-1} + \mathcal{C}_k^{-1}(\mathcal{R} - \mathcal{J}_k \delta\mathcal{U}_{l-1}),\ l \le \nu_1$$
$$\mathcal{Z}_1 = MG(k-1, \mathbf{0}, \mathcal{I}_k^{k-1}(\mathcal{R} - \mathcal{J}_k \delta\mathcal{U}_{\nu_1}))$$

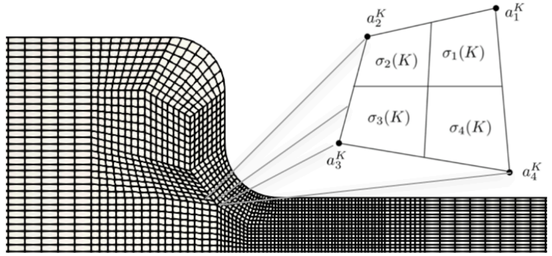

$$\delta\mathcal{U}_l = \delta\mathcal{U}_{l-1} + \mathcal{C}_k^{-1}(\mathcal{R} - \mathcal{J}_k \delta\mathcal{U}_{l-1}),\ l \le \nu_2$$
$$MG(k, \delta\mathcal{U}_0, \boldsymbol{\mathcal{R}}) = \delta\mathcal{U}_{\nu_1} + \mathcal{I}_{k-1}^{k} \mathcal{Z}_2$$

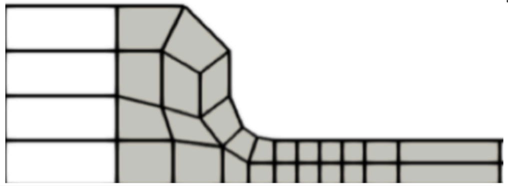

$$MG\,(1, \delta\mathcal{U}_0, \mathcal{R}) = \mathcal{J}_1^{-1}\mathcal{R}$$

- **Transfer between FE spaces**

$$\boldsymbol{\mathcal{I}}^{\tilde{\mathbf{u}}}_{k,k-1} = \boldsymbol{M}_{k-1}^{-1} \left(\boldsymbol{\mathcal{I}}^{\tilde{\mathbf{u}}}_{k-1,k}\right)^T \boldsymbol{M}_k$$
$$\boldsymbol{\mathcal{I}}^{p}_{k-1,k} = \boldsymbol{M}_k^{-1} \boldsymbol{M}_{k-1}$$

$$\left[\boldsymbol{\mathcal{I}}^{\tilde{\mathbf{u}}}_{k-1,k}\right]_{ij} = \mathcal{N}_j^k(\varphi_i^{k-1})$$
$$\boldsymbol{\mathcal{T}}^p = \boldsymbol{M}_k^{-1} \boldsymbol{M}_{k-1}$$

- **Coarse grid solver**

$$\mathcal{R}_{k-1} = \left(\boldsymbol{\mathcal{I}}^{\tilde{\mathbf{u}}}_{k-1,k}\right)^T \mathcal{R}_k$$
$$\mathcal{J}^{\tilde{\mathbf{u}}}_{k-1} = \left(\boldsymbol{\mathcal{I}}^{\tilde{\mathbf{u}}}_{k-1,k}\right)^T \mathcal{J}^{\tilde{\mathbf{u}}}_k \boldsymbol{\mathcal{I}}^{\tilde{\mathbf{u}}}_{k,k-1}$$

- **LMPSC**

$$\mathcal{U}^{k+1} = \mathcal{U}^k - \omega_k \sum_{K \in \mathcal{T}_h} \boldsymbol{\mathcal{P}}_K \left(\boldsymbol{\mathcal{P}}_K^{\mathrm{T}} \left(\frac{\partial \mathcal{R}(\mathcal{U}^k)}{\partial \mathcal{U}}\right) \boldsymbol{\mathcal{P}}_K\right)^{-1} \boldsymbol{\mathcal{P}}_K^{\mathrm{T}} \mathcal{R}(\mathcal{U}^k).$$

Type-transitions investigation

Axial flow experiment and numerical simulations in the Couette device

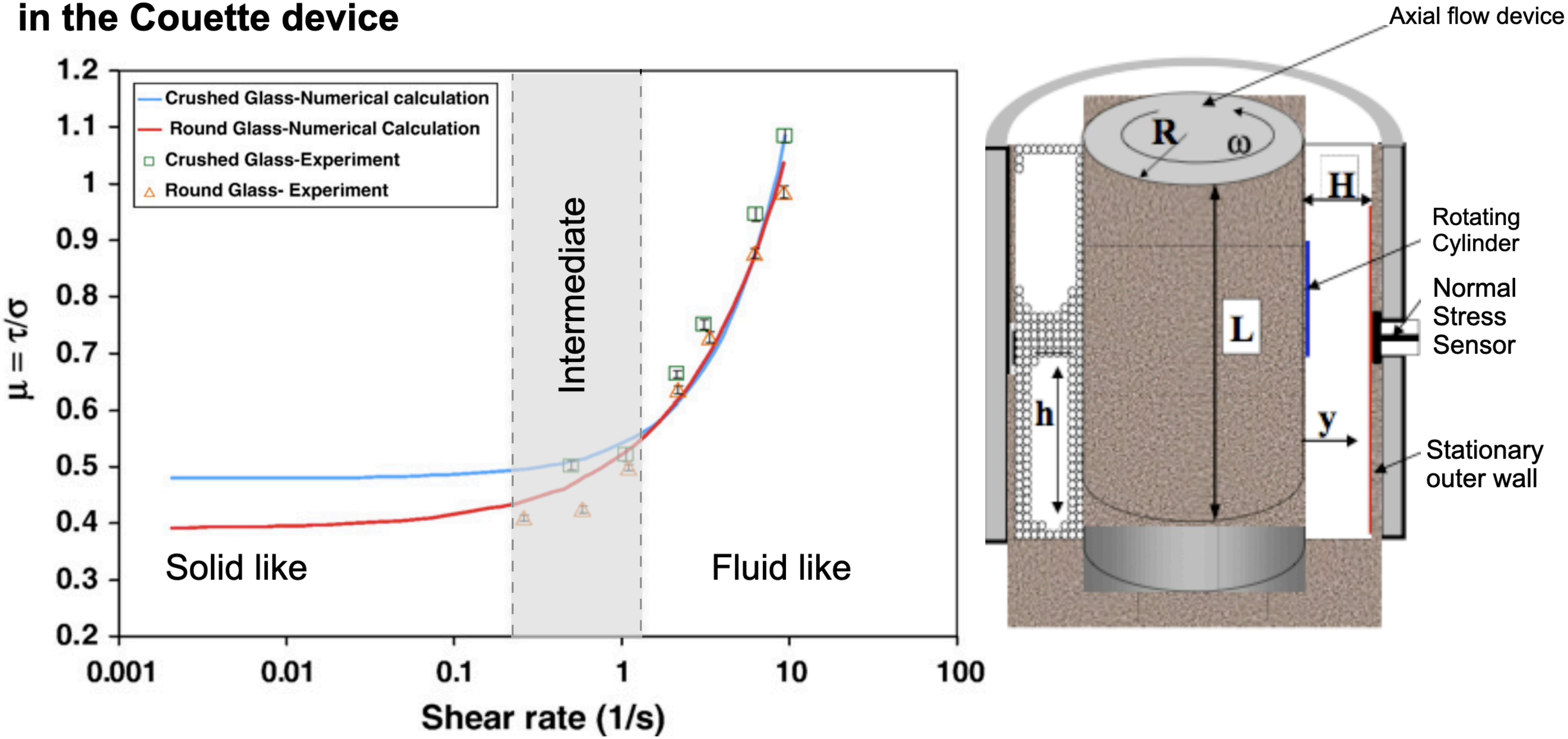

✓ **The material can transit from the solid like to liquid like regions as the shear rate is increased**

Solid / Liquid & liquid / solid type-transitions investigation w.r.t. thixotropy !

- **Torque calculation**

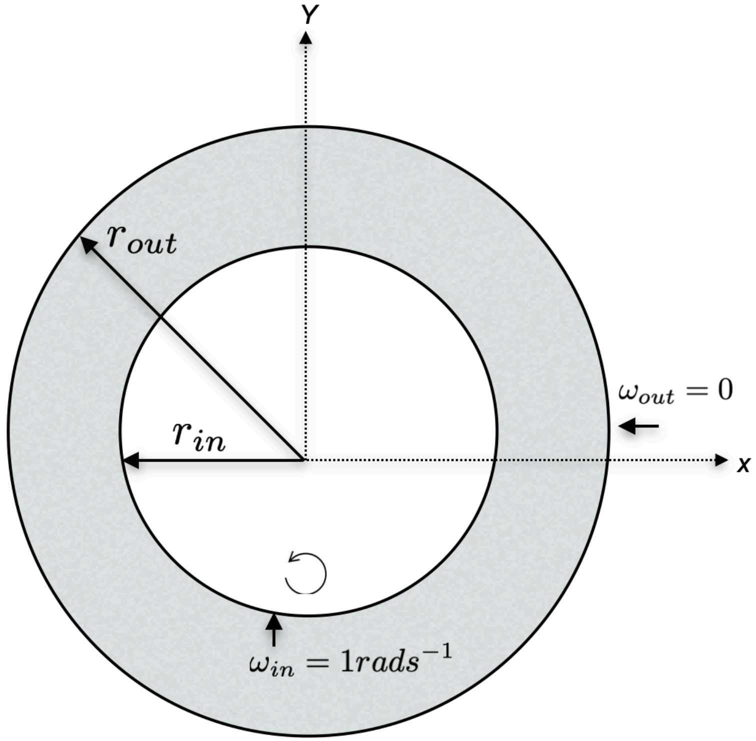

$$M = -\oint_S (X - X_0) T_{ij} \vec{n} dS$$

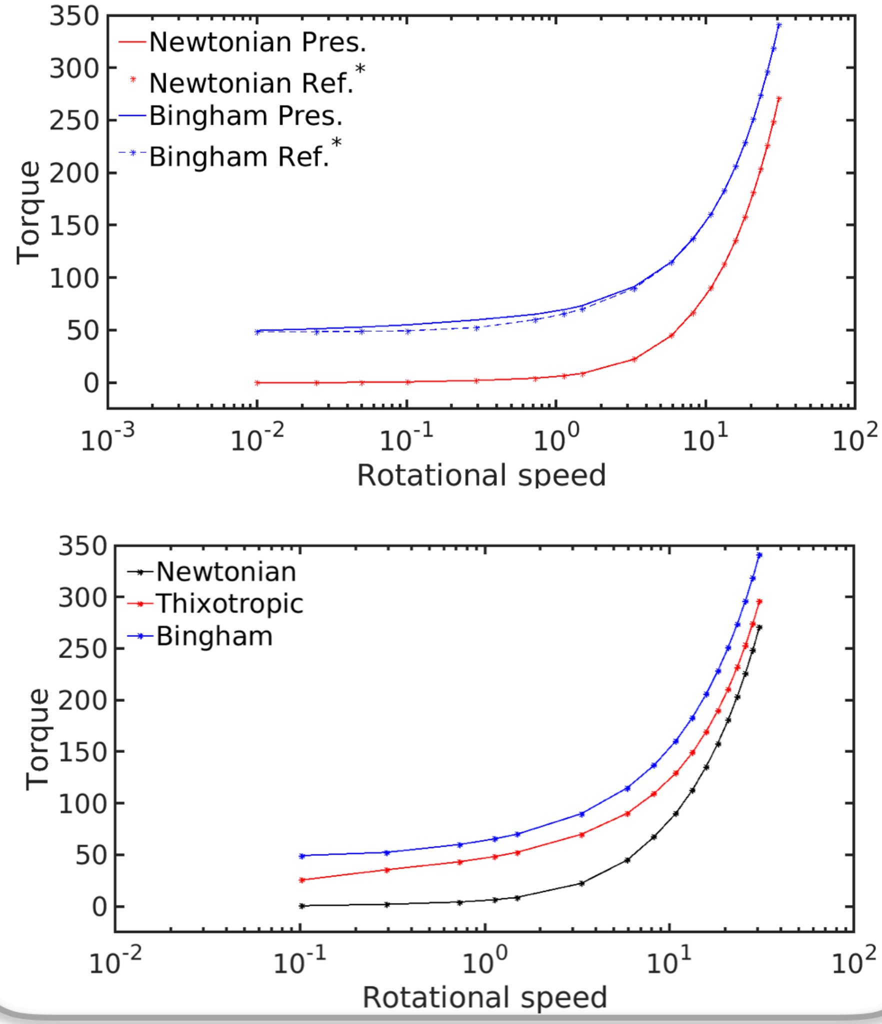

- ✓ **Torque calculation for Non-thixotropic flow**
- ✓ **Thixotropic flow is encompassed between Newtonian flow and Bingham plastic flow, as predicted by the Houska's model, allowing for transitions' type study**

Thixo-viscoplastic flow in Couette

technische universität dortmund

- **Microstructure solutions in a Couette device w.r.t breakdown parameter**

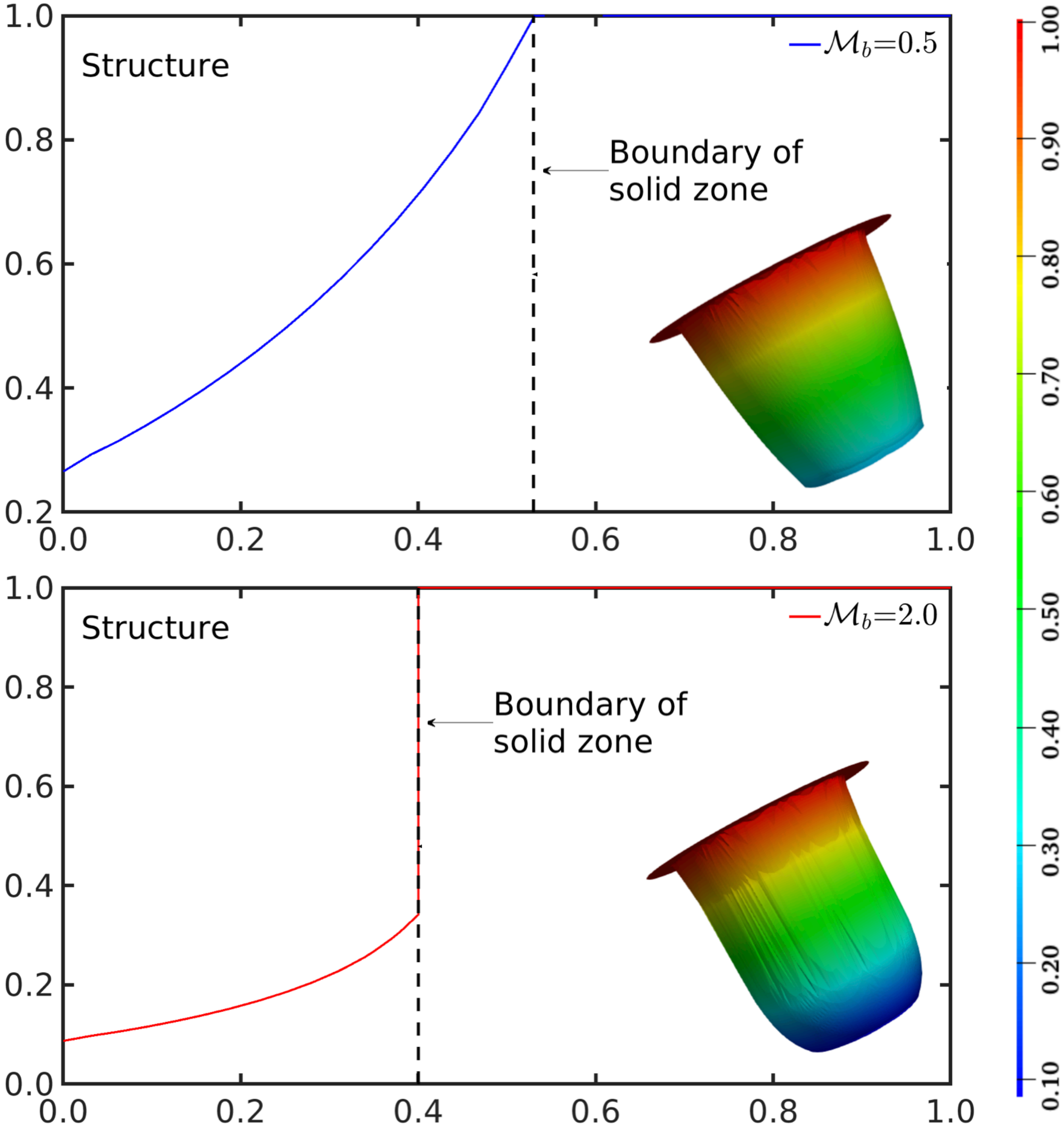

Thixo-viscoplastic flow in Couette

- **Cut-line positions $c; c \in [0, 2\pi]$ in a Couette device w.r.t breakdown parameter**

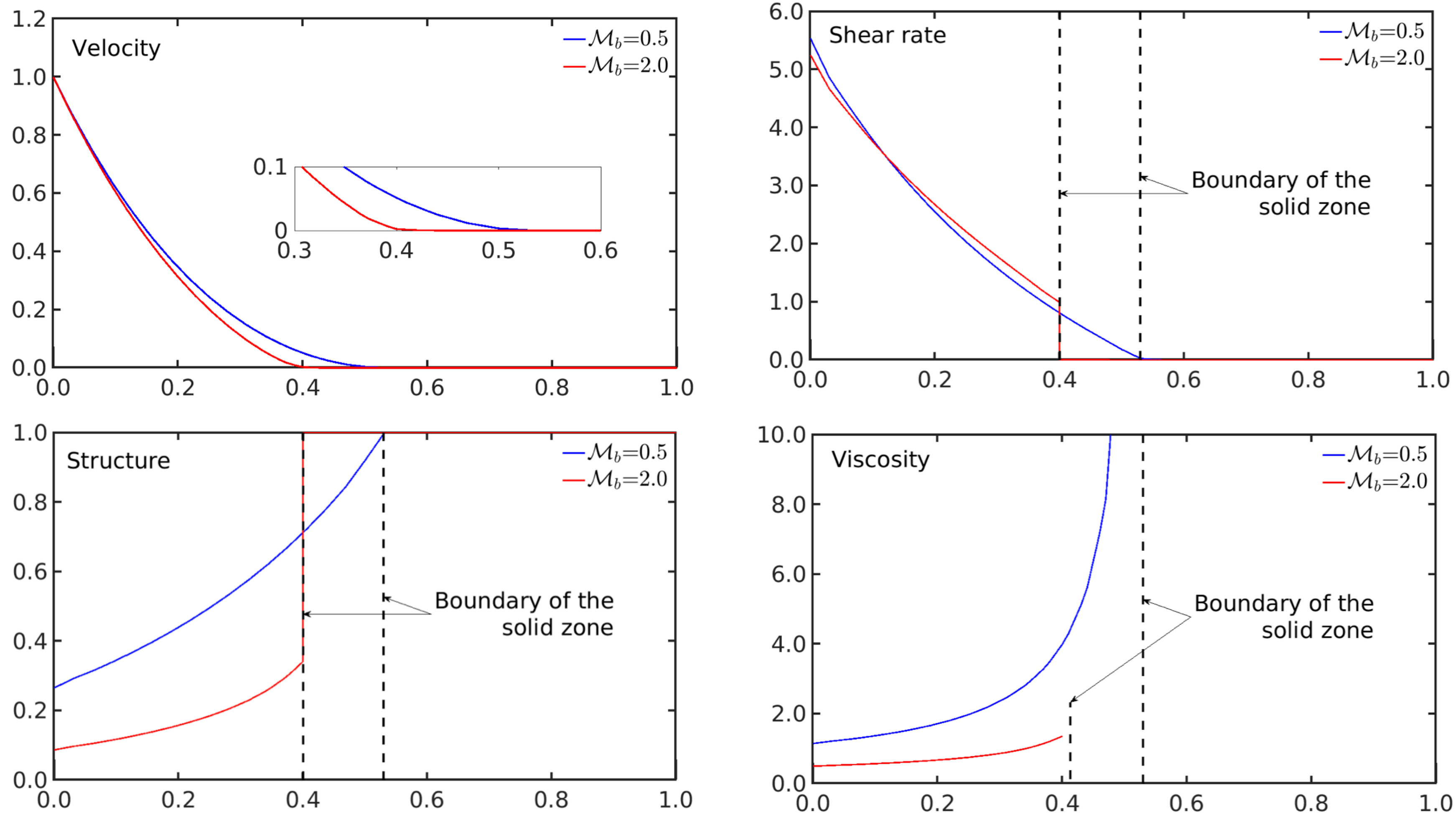

- ✓ **Shear Localization & shear banding transition types w.r.t breakdown parameter**
- ✓ **Transition point for shear-rate and structure parameter match with velocity**
- ✓ **Structure parameter predicts the shape and extent of rigid zones**

- 2D-FEM simulation results for thixo-viscoplastic flow- validation of 1D tool
- Specifying the "unidirectional profiles as boundary Data" in 2D for contraction domain

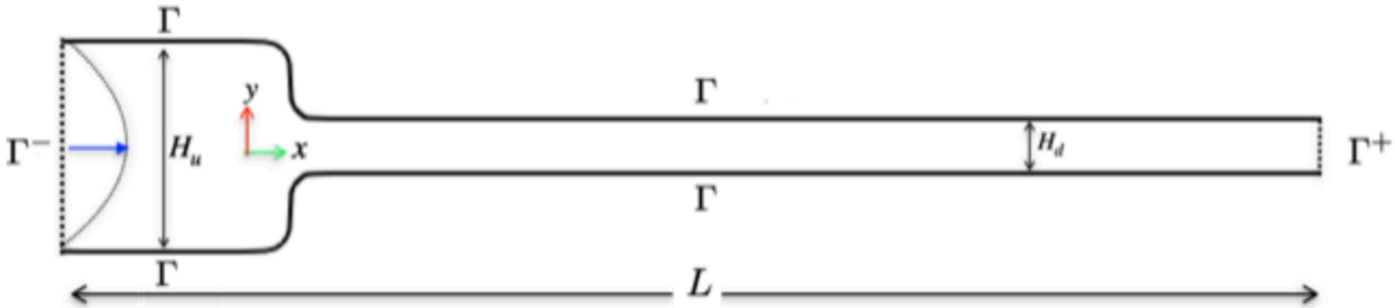

Mesh

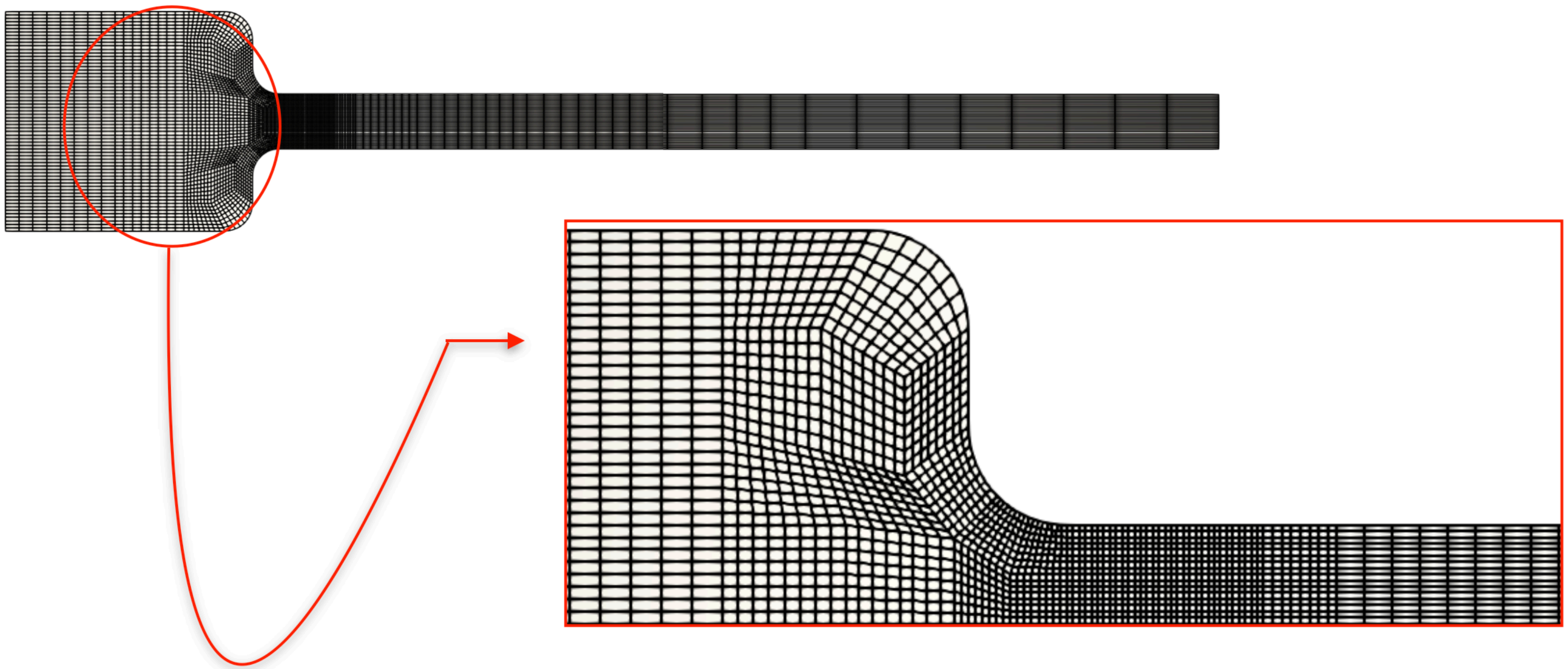

- **Interplay of thixotropy and plasticity**

- **Material microstructure**

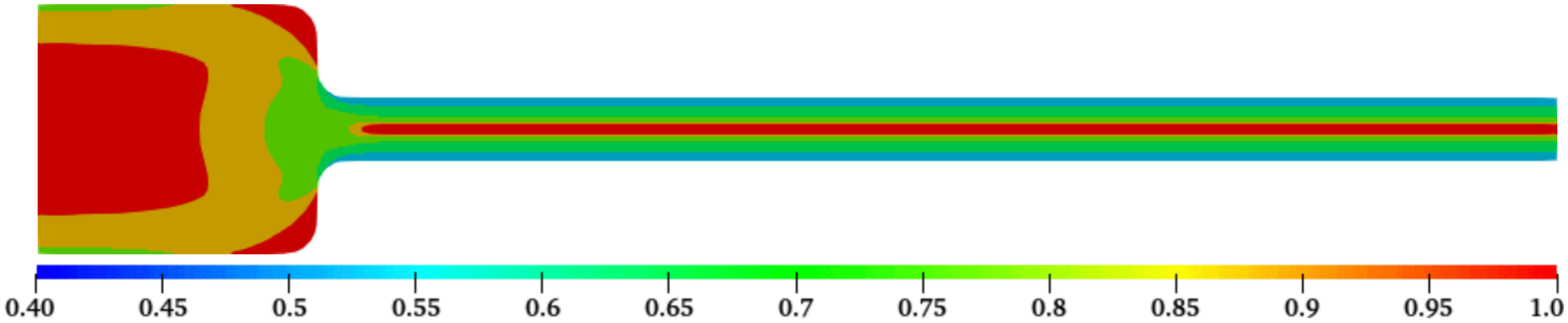

- **Flow distribution**

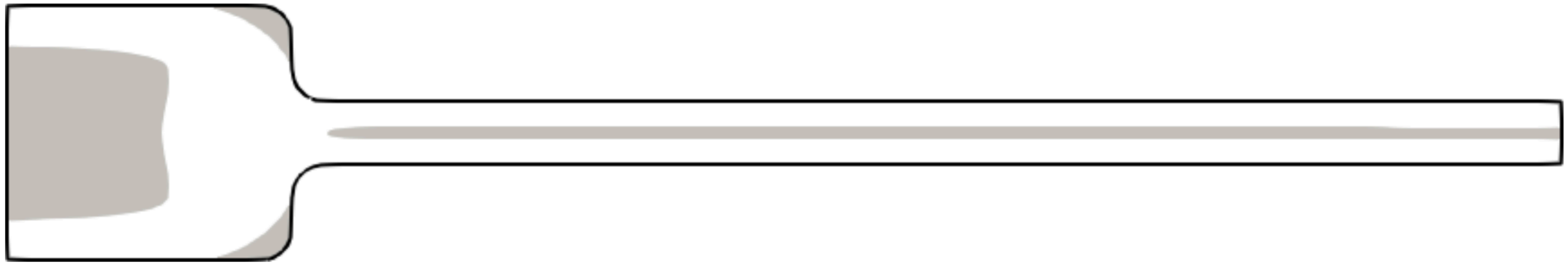

✓ **Symbiotic interplay of thixotropic and plastic phenomena**

- **Material microstructure w.r.t. breakdown**

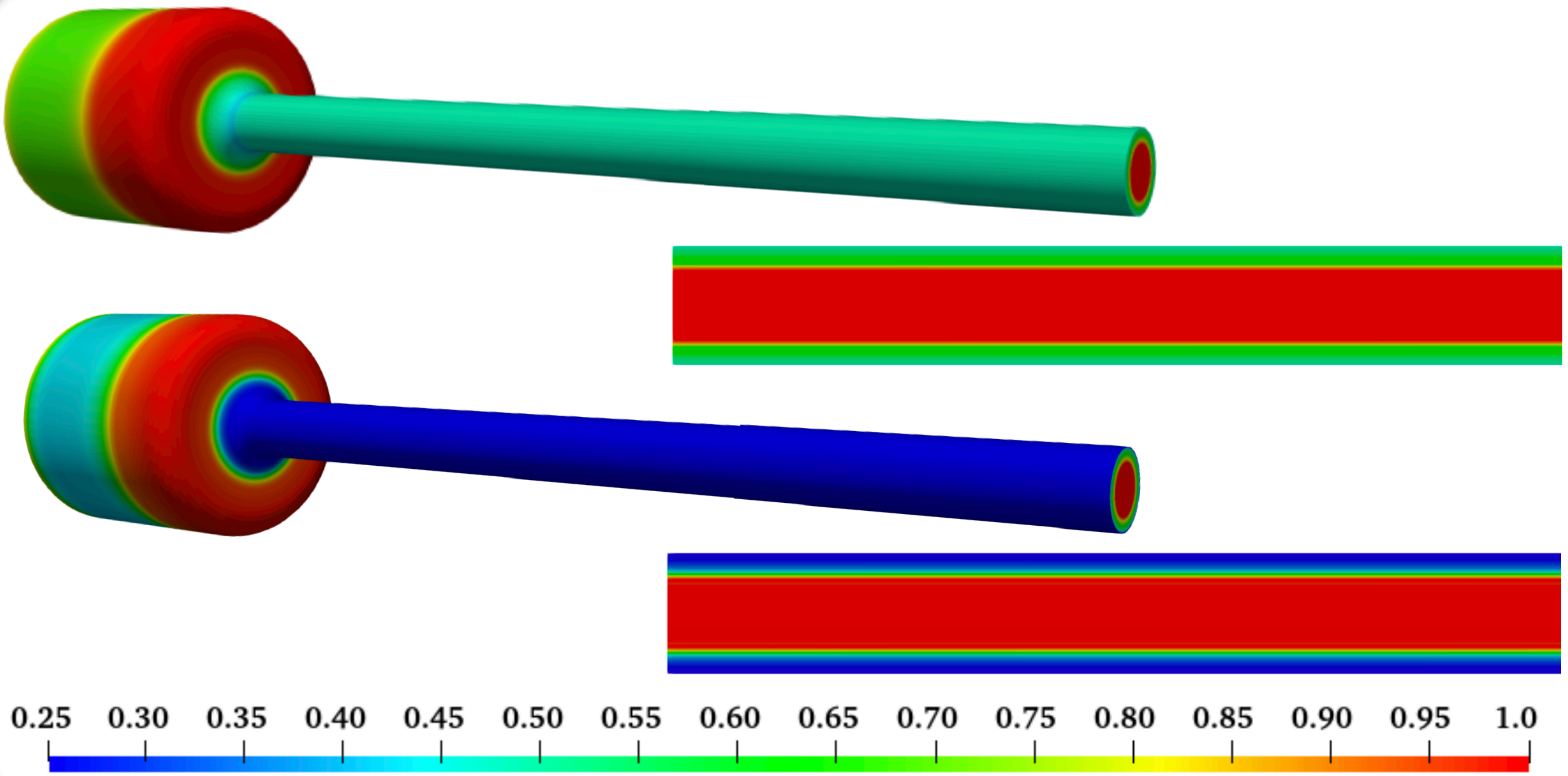

- **Inherent thixotropy speed-up the breakdown**

✓ **Appearance of more breakdown layers**
✓ **Applications: restart pressure in pipelines can be optimised**

Summary

Monolithic geometric multigrid FEM solver for thixo-viscoplastic flows is developed based on

- ✓ **Quasi-Newtonian modelling approach**
- ✓ **Higher order stabilized FEM to**
    - **enhance weak norm for microstructure**
    - **counterbalance regularization impact**
- ✓ **Monolitic Newton-multigrid solver using**
    - **global adaptive discrete Newton's method**
    - **geometric multigrid with LMPSC**

To analyze thixo-viscoplastic Couette and contraction flows

[1] Ouazzi, A., Begum, N.,Turek, S., Newton-Multigrid FEM Solver for the Simulation of Quasi-Newtonian Modeling of Thixotropic Flows, 700, *Numerical Methods and Algorithms in Science and Engineering*, 2021.

[2] Begum, N., Ouazzi, A., Turek, S., Finite Element Methods for the simulation of thixotropic flow problems, *in: 9th edition of the International Conference on Computational Methods for Coupled Problems in Science and Engineering (COUPLED PROBLEMS 2021)*.

[3] Begum, N., Ouazzi, A., Turek, S., Monolithic Newton-multigrid FEM for the simulation of thixotropic flow problems, *Kaliske, M., 21, 1, 92nd Annual Meeting of the International Association of Applied Mathematics and Mechanics (GAMM), Wiley-Interscience*, https://doi.org/10.1002/pamm.202100019, 2021.

[4] Begum, N., Ouazzi, A., Turek, S. *Monolithic Finite Element method for the simulation of thixo-viscoplastic flows*, Book of Extended Abstracts of the 6th Eccomas Young Investigators Conference, doi.org/10.4995./YIC2021.2021.12250, 2021

[5] Begum, N., Ouazzi, A., Turek, S., *FEM analysis and Newton-multigrid solver for thixo-viscoplastic flow problems,* ECCOMAS, 10.23967/eccomas.2022.119, 2022.

[6] Begum, N., Ouazzi, A., Turek, S., *FEM simulation of thixo-viscoplastic flow problems;* Error analysis, Ergebnisberichte des Instituts für Angewandte Mathematik Nummer 656, Fakultät für Mathematik, TU Dortmund, 653, 2022.

[7] Jenny, M., Kiesgen de Richter, S., Louvet, N., Skali-Lami, S. Dossmann, Y. ,Taylor-Couette instability in thixotropic yield stress fluids. *Phys. Rev. Fluids* (2017) 2:023302–023323.

[8] Kheiripour Langroudi, M., Turek, S., Ouazzi, A., Tardos, G.I. An investigation of frictional and collisional powder flows using a unified constitutive equation,*Powder Technology,* 197, 91-101, 2010.

[9] Ouazzi, A. *Finite Element Simulation of Nonlinear Fluids: Application to Granular Material and Powder*, Shaker Verlag Aachen, ISBN 3-8322-5201-0, 2006.

Acknowledgments

- We acknowledge the funding provided by the “Bundesministerium für Wirtschaft und Klimaschutz aufgrund eines Beschlusses des Deutschen Bundestages” through “ AiF-Forschungsvereinigung: Forschungs-Gesellschaft Verfahrens-Technik e. V. - GVT” under the IGF project number “20871 N”
- We acknowledge the funding provided by the “Deutsche Forschungsgemeinschaft (DFG, German Research Foundation) - 446888252”
- We acknowledge the support by LSIII and LiDO3 team at ITMC, TU Dortmund University, Germany

lehrstuhl für angewandte mathematik und numerik

it & medien centrum

Deutsche Forschungsgemeinschaft

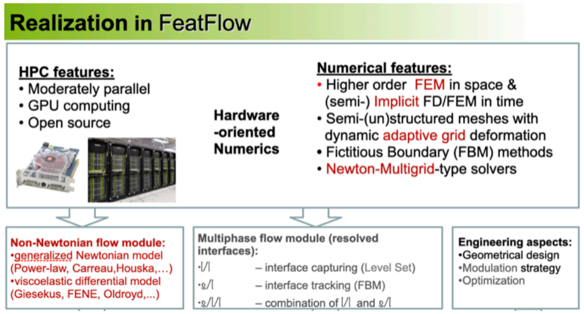

Bundesministerium für Wirtschaft und Klimaschutz

Das Kunststoff-Zentrum

ALLIANZ INDUSTRIE FORSCHUNG